Comparing Lipid Photo-Cross-linking Efficacy of Penetratin Analogues Bearing Three Different Photoprobes: Dithienyl Ketone, Benzophenone, and Trifluoromethylaryldiazirine

Chen-Yu Jiao, Isabel D. Alves, Vanessa Point, Solange Lavielle, Sandrine Sagan, and Gérard Chassaing*

UPMC Paris 06 - ENS - CNRS, UMR 7203, Laboratoire des BioMolécules, FR 2769 Chimie Moléculaire, Université Pierre et Marie Curie, Case courier 182, 4, Place Jussieu, 75252 Paris Cedex 05, France. Received October 26, 2009; Revised Manuscript Received January 4, 2010

Photoactivatable penetratin analogues bearing three different photoprobes, which do not disturb the membranotropic properties of the peptides, have been tested for their photo-cross-linking efficacy in glycerol and lipid media. In the case of glycerol, photo-cross-linking was observed, whereas in the case of SDS (used as a membrane model system), the dynamics of the SDS/penetratin assemblies and the photosensitizer properties of the probes prevented the cross-linking between the peptide and SDS. Bilayers of DMPG were partially photo-cross-linked by the penetratin analogues containing either a benzophenone or a trifluoromethylaryl-diazirine, whereas dithienyl ketone acted exclusively as a photosensitizer. The characterization by MALDI-TOF mass spectrometry of the photoadducts formed after irradiation required basic hydrolysis of DMPG for an efficient capture of the biotinylated peptide analogues with streptavidin-coated magnetic beads. MALDI-TOF analysis of the photoadducts between the photoactivatable penetratin and DMPG allowed an unambiguous identification of the covalent bond formed with the lipids. Altogether, we show herein that the efficacy of the lipid photo-cross-linking depends on the environment, the dynamics of the supramolecular assembly, and the physicochemical properties of the photoprobe.

INTRODUCTION

The formation of a covalent bond, after irradiation of a photoactivatable molecule, is a commonly used strategy for linking ligands to both hard and soft surfaces (*1*−*3*). For that purpose, four types of photoactivatable aryl reagents are mainly used: aryldiazonium salts, diazoaryl, trifluoromethylaryldiazirines, and phenylketone (*4*). To study by photolabeling the interaction topography between a ligand and its protein partner, the specifications are more stringent, since the photoactivatable probe should be located in the immediate vicinity of the binding domain and, upon irradiation, should form promptly a covalent bond with the protein (*5*). The bioconjugated construct possesses different "moieties". A peptide ligand usually includes an adequately positioned photoprobe in its sequence, together with a recognition moiety (e.g., biotin) used to purify the covalent complex from the incubation mixture (*6*). The tricky step is often the correct rational design of a ligand that retains a high and specific affinity for the protein partner.

Upon irradiation, the photoactivatable probe is transformed into a highly reactive radical species that can abstract a hydrogen atom present in its close environment within the protein binding site. Thus, an important aspect to consider is the reactivity of the chosen photoreactive probe, which must lead to molecular species reactive enough within the time scale of the ligand−protein complex half-life time. Generally, the binding affinity of peptide ligands for their receptor is high (in the nanomolar range), corresponding to formation of complexes with a half-life time in the minutes range. This corresponds to a much longer time than what is mostly observed for reactive species ($t_{1/2}$ values around microseconds or shorter). Even in "host−guest" complexes such as benzophenone/cyclodextrin or transmembrane peptide/phospholipids in which the affinity is low ($t_{1/2}$ value around milliseconds), the irradiation-assisted cross-linking was not inhibited (*7, 8*). The confinement of the reactive species and the "freezing" of internal movements of both the ligand and the receptor (or guest molecule) within these complexes restrain the intrinsic mobility of both molecules. Thus, it is believed that the covalent bond formation likely represents a snapshot of the interaction.

The goal of the present study was to test the feasibility and the limitations of photochemistry in the analysis of the interaction(s) of a cationic peptide with a highly dynamic system, such as plasma membranes constituted of a large range of molecular components and supramolecular assemblies. Plasma membranes are considered a mosaic of coexisting domains: the fluid lipid matrix in disordered phase, lipid ordered domains (rafts), nanodomains associated with different types of proteins (caveolins, clathrin, actin, receptors, protein channels, etc.) and some transient confinement zones (*9, 10*). The overall dynamic of this mosaic is considered to occur in the nano- to milliseconds time scale (*11*). However, if one considers the rotation around a C−C bond or along the membrane axis and the aliphatic chain wobbling in the disordered phase, the correlation times of phospholipids greatly vary from 10^{-12} to 10^{-7} s. The correlation time for the lateral diffusion is greater than 10^{-5} s and supramolecular assemblages occur starting from very small rafts (diameter <10 nm) to larger ones (from 30 to 230 nm) in time scales of 10^{-3} s (*12, 13*). Photoactivatable lipids have been used to probe the interaction within lipids (*14*). Modifications of lipids by highly reactive radicals, such as oxygen-derived species, have also been reported (*15*). Herein, we address the question of the photochemistry strategy as a reliable method to study peptide/lipid interaction.

Penetratin, (corresponding to helix-3 of Antennapedia homeodomain: Arg-Gln-Ile-Lys-Ile-Lys-Phe-Gln-Asn-Arg-Arg-Met-Lys-Trp-Lys-Lys), is a cationic membranotropic peptide,

* Corresponding author. Dr. Gérard Chassaing, UMR 7203, Laboratoire des BioMolécules, Case courier 182, 4, Place Jussieu, 75252 Paris Cedex 05, France. Fax: +33 1 44 27 71 50. Tel: +33 1 44 27 32 61. E-mail: gerard.chassaing@upmc.fr.

10.1021/bc900466q © 2010 American Chemical Society
Published on Web 01/20/2010

Scheme 1. Structures of the Three Photoactivatable Probes (X = Bz, DTK, or TMD) Attached to Lys48 within the Sequence of Penetratin[a]

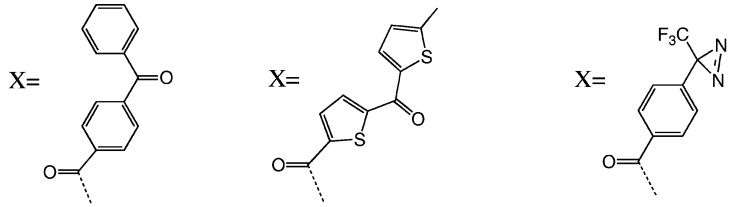

Benzophenone (Bz) Dithienylketone (DTK) Trifluoromethylaryldiazirines (TMD)

Biotin-$(Gly)_4$-Arg^{43}-Gln-Ile-Lys-Ile-Lys^{48}-Phe-Gln-Asn-Arg-Arg-Met(O)-Lys-Trp-Lys-Lys^{58}-$CONH_2$

NH-X with X = Bz Pen(Lys48Bz): MW = 2864

Biotin(O_2)-$(Gly)_4$-Arg^{43}-Gln-Ile-Lys-Ile-Lys^{48}-Phe-Gln-Asn-Arg-Arg-Met-Lys-Trp-Lys-Lys^{58}-$CONH_2$

NH-X with X = DTK or TMD Pen(Lys48DTK): MW = 2906; Pen(Lys48TMD): MW = 2886

[a] The three penetratin analogues are modified at the N-terminus by Biotinylated-$(Gly)_4$ and are abbreviated herein as Pen(Lys48Bz), Pen(Lys48DTK), and Pen(Lys48TMD).

a prototype of cell-penetrating peptide, which is able to enter eukaryotic cells without cytotoxity, and which presents antimicrobial activities in some prokaryotic cells (*16, 17*). Even if parallel orientations of penetratin to bilayer were clearly established by various biophysical methods, a direct translocation has been shown as one of the entry mechanism of penetratin in eukaryotic cells (*18*). As Trp48 was found located in the hydrophobic area of phospholipids (*19, 20*), we have substituted this residue by an acylated lysine on the side-chain with three different photoprobes: phenylketone, dithienylketone, or trifluoromethylaryldiazirine (Scheme 1). As we have already described for other studies (*18, 21*−*23*), these photoactivatable penetratin analogues were also functionalized with biotin, separated from the penetratin sequence by a spacer of four glycines, which allows an easy purification through streptavidin-grafted magnetic beads before MALDI-TOF mass spectrometry analysis. The influence of the different photoprobes on the membranotropic properties of penetratin has been analyzed by monitoring their effect on lipid phase transition using differential scanning calorimetric (DSC). Since electrostatic interactions have been shown to play an important role in lipid interaction with penetratin (*24, 25*) large multilamellar vesicles (MLVs) made of dimyristoylphosphatidylglycerol (DMPG) were used as models of the highly dynamic cell membrane. The photochemical behavior of the different peptide analogues has been analyzed in water, glycerol, and sodium dodecyl sulfate (SDS) as models of aqueous, polar headgroups and lipophilic environment of the membrane, respectively. DMPG MLVs were irradiated with the photoactivatable analogues (above the phase transition temperature) and the resulting photoadducts analyzed by mass spectrometry to compare their cross-linking efficacy.

EXPERIMENTAL PROCEDURES

DMPG was purchased from Genzyme (Switzerland) and was used without further purification. 4-Carboxybenzophenone and 4-(trifluoroacetyl)benzoic acid were purchased from Aldrich and Apollo Scientific Limited, respectively. The 5-carboxy-5′-methyl-2,2′-dithienylketone was a generous gift, from the "Laboratoire d'Ingénierie Moléculaire et Biochimie Pharmacologique", Université Paul Verlaine, Metz, France.

Syntheses of Photoactivatable Probes. *4-[1-(trifluoromethyl)-3H-diazirinin-3-yl]benzoic Acid.* The synthesis of 4-[1-(trifluoromethyl)-3*H*-diazirinin-3-yl]benzoic acid was based on a series of reactions already used for this type of photoprobes (*26, 27*).

4-(trifluoroacetyl)benzoic tert-Butyl Ester **1.** 4-(Trifluoroacetyl) benzoic *tert*-butyl ester **1** was prepared from *tert*-butyl alcohol and 4-(trifluoroacetyl)benzoic acid using anhydrous magnesium sulfate and sulfuric acid. To a suspension of $MgSO_4$ (92 mmol) in CH_2Cl_2 (100 mL), H_2SO_4 (23 mmol) was added dropwise After 15 min of stirring, *tert*-butyl alcohol and 4-(trifluoroacetyl)benzoic acid were added. The mixture was stirred for two days and the reaction was quenched by addition of saturated $NaHCO_3$ (170 mL). The extraction with CH_2Cl_2 led to 10 mmol of pure 4-(trifluoroacetyl)benzoic *tert*-butyl ester. R_F (cyclohexane/ethyl actetate, 8/2) = 0.3. ^{1}H NMR ($CDCl_3$), δ: 1.62 (s, 9H), 8.13 (s, 4H). The unreacted starting material was recovered after acidification of the aqueous phase and extraction with CH_2Cl_2.

4-(2-Trifluoroethanoneoxime)benzoic tert-Butyl Ester **2.** To a stirred mixture of hydroxylamine hydrochloride (8 mmol) and NaOH (8 mmol) in 33 mL of boiling ethanol, compound **1** (8 mmol in EtOH, 4 mL) was added dropwise. After refluxing for 3 days, ether was added, and the organic layers were washed with 0.01 N HCl (3×) and with water (3×). R_F ($CHCl_3$) = 0.25. ^{1}H NMR ($CDCl_3$), δ: 1.6 (s, 9H), 7.59 (d, 2H), 8.10 (q, 2H), 8.38 (s, broad 1H).

4-(2-Trifluoroethanone-O-(p-tolylsulfonyl)oxime)benzoic tert-Butyl Ester **3.** A mixture of compound **2** (19 mmol) and of *p*-sulfonyl chloride (38 mmol) in dry pyridine (30 mL) was refluxed for 3 days. After solvent evaporation, the pure product (yield 73%) was obtained after flash chromatography, (cyclohexane/ethyl acetate, 95/5). R_F ($CHCl_3$) = 0.66. ^{1}H NMR ($CDCl_3$), δ: 1.6 (s, 9H), 2.48 (s, 3H), 7.41 (t, 4H), 7.86 (d, 2H), 8.06 (d, 2H).

4-(Trifluoromethyldiaziridine)benzoic tert-Butyl Ester **4.** Compound **3** (2 mmol) was introduced in a Parr Instrument of 0.3 L capacity, then liquid ammonia (20 g) was condensed after cooling the autoclave in liquid nitrogen for 15 min. The mixture was stirred for two days. After evaporation, the pure product (yield 88%) was obtained after flash chromatography using CH_2Cl_2. R_F ($CHCl_3$) = 0.5. ^{1}H NMR ($CDCl_3$), δ: 1.6 (s, 9H), 2.25 (d, 1H), 2.80 (d, 1H), 7.58 (d, 2H), 8.05 (d, 2H).

4-[1-(Trifluoromethyl)-3H-diazirinin-3-yl]benzoic tert-Butyl Ester **5.** Compound **4** (1 mmol) was mixed with freshly prepared Ag_2O (5 mmol). After stirring for 3 h in the dark, the mixture was filtered on Celite and purified by flash chromatography using cyclohexane. R_F ($CHCl_3$) = 0.75. ^{1}H NMR ($CDCl_3$), δ: 1.59 (s, 9H), 7.24 (d, 2H), 8.01 (d, 2H).

4-[1-(Trifluoromethyl)-3H-diazirinin-3-yl]benzoic Acid **6.** Compound **5** (10 mmol) was stirred with TFA (50 mmol) in CH_2Cl_2 (10 mL). The reaction was completed after two hours stirring, leading after usual workup to compound **6**. R_F ($CHCl_3$) = 0.2. ^{1}H NMR (DMSO), δ: 7.40 (d, 2H), 8.06 (d, 2H), 13.34 (s, 1H).

Synthesis of Penetratin Analogues. The penetratin analogues [Lys^{48}(Bz)]Penetratin, [Lys^{48}(DTK)]Penetratin, and [Lys^{48}(TMD)]-Penetratin abbreviated as Pen(Lys48Bz), Pen(Lys48DTK), and Pen(Lys48TMD), respectively, and modified on Lys48 (number 48 corresponding to the Trp position in the sequence of the *Antennapedia* homeodomain (*28*) were synthesized by solid-phase methodology on a ABI 431 Synthesizer, using either a Rink amide resin or Rink amide MBHA resin by Fmoc or Boc strategies, respectively. Lys48 side chain was protected either by Fmoc or Dde protecting groups for the Boc and Fmoc strategies, respectively. After selective removal of the protecting group, the free amine of Lys48 was acylated either by 4-carboxybenzophenone, 5-carboxy-5′-methyl-2,2′-dithienylketone or 4-[3-(trifluoromethyl)-3*H*-diazirinin-3-yl]benzoic acid, using DCC/HOBt for the activation. The subsequent Ile45 was then introduced manually. The other amino acids were coupled on the synthesizer using standard protocols of Boc and Fmoc chemistries and amino acid activation with DCC/HOBt in NMP. After removal of the last protecting group from the N-terminal glycine, the peptides were biotinylated in NMP, as already described (*18, 21*−*23*). The resins were washed with NMP, CH_2Cl_2, and MeOH and dried under vacuum. The peptides were cleaved from the resin with TFA/H_2O/TIS (Fmoc strategy) (95/2.5/2.5) or HF/anisole (Boc strategy). The crude peptides were lyophilized and purified by RP-HPLC. The peptides were characterized by MALDI-TOF mass spectrometry leading to *m*/*z* 2864 for Pen(Lys48Bz), 2908 for Pen(Lys48DTK), and 2886 for Pen(Lys48TMD).

Differential Scanning Calorimetry. The calorimetry was performed on a high-sensitivity differential scanning calorimeter (Calorimetry Sciences Corporation). A scan rate of 1 °C/min was used, and there was a delay of 10 min between sequential scans in a series that allow for thermal equilibration. Data analysis was performed with the fitting program *Cpcalc* provided by CSC and plotted with *Igor*. DMPG (1 mg/mL) was used at peptide/lipid ratio of 1/25. Samples containing the peptide alone, dissolved in buffer at similar peptide concentrations, exhibited no thermal events over the temperature range 0−100 °C. This indicates that the peptides do not denature over this temperature range and that the endothermic events observed in this study arise solely from phase transitions of the phospholipid vesicles. A minimum of at least three to four heating and cooling scans were performed for each analysis depending on whether or not the spectra was reproducible.

Photolabeling. The sample of Pen(Lys48Bz), Pen(Lys48DTK), or Pen(Lys48TMD) dissolved at micromolar concentration in water or glycerol (500 μL) was irradiated on ice for 1 h at 365 nm with an UV light (HPR 125-W) located between 6 to 10 cm from the Eppendorf tube corresponding to a surface area of 0.39 cm^2. Then, 1 μL of the irradiated sample was deposited on the sample holder for direct MALDI-TOF mass spectrometry analysis.

DMPG (1 μM in 20 mM ammonium acetate buffer at pH 7.5) was mixed with Pen(Lys48Bz), Pen(Lys48DTK), or Pen(Lys48TMD) at 1/10 peptide/lipid ratio. Theses samples were irradiated on ice for 1 h, under the conditions described above, followed by a basic hydrolysis in MeOH/H_2O (50/50) using NaOH (0.1 M) at 37 °C overnight. After neutralization with acetic acid, the methanol was evaporated before affinity purification.

Purification with Streptavidin-Coated Magnetic Beads. The hydrolyzed sample containing 0.1% of Triton was incubated with streptavidin-coated magnetic beads (100 μg, Dynabeads M280, Dynal) for 30 to 60 min under gentle agitation. The washing steps (5× each) were performed with (1) buffer (Tris pH 7, 50 mM) containing 0.1% SDS, (2) 50 mM Tris pH 7, (3) NaCl 1 M, and (4) H_2O/ACN 50/50. The same procedure was used for the experiments performed in SDS, excepted that no Triton was added during the incubation step.

MALDI-TOF Mass Spectrometry Analysis. The photoadducts were eluted from the magnetic beads with the 2,5-dihydroxybenzoic acid (DHB) matrix, in 1:1 (v/v) CH_3CN/H_2O (1% phosphoric acid) used for MALDI analysis. After 10 min incubation, 1 μL of bead-free supernatant was deposited on the sample holder.

Quantification by MALDI-TOF Mass Spectrometry. After irradiation in glycerol of deuterated Pen(Lys48Bz) (penetratin analogue with four deuterated glycines), a known amount (2 nmol) of hydrogenated Pen(Lys48Bz) (with four 1*H*-glycines) was added to the medium. The photoadduct was then purified by incubating the mixture with streptavidin-coated magnetic beads for 30 to 60 min under gentle agitation. After elution of all biotinylated peptides (photoadduct or free peptide) with the matrix as described above, 1 μL of bead-free supernatant was deposited on the sample holder. The ratio of the ^{1}H/^{2}H MH+ *m*/*z* signals allowed the quantitative determination of the starting peptide that remained intact after irradiation.

RESULTS

Hydrophobic Character of Penetratin Analogues. The modification of the hydrophobic/hydrophilic balance induced by the photoprobes on the behavior of these penetratin analogues can be related to the concentration of acetonitrile required to elute the corresponding peptides by HPLC (in mixture of acetonitrile water 0.1% of TFA). The concentrations required correspond to 32.4% CH_3CN for Pen(Lys48Bz), 21.5% CH_3CN for Pen(Lys48DTK), and 32% CH_3CN for Pen(Lys48TMD), leading to the following hydrophobic scale: Pen(Lys48DTK) > Pen(Lys48Bz) ≈ (Lys48TMD).

Effect of the Medium on the Photochemical Properties of the Different Photoprobes. Ammonium acetate buffer, glycerol, and sodium dodecyl sulfate (SDS) were used as models of the membrane interface. The crude products obtained after irradiation (1 h) at 365 nm of these photoactivatable penetratin analogues within one of the media were analyzed by MALDI-TOF mass spectrometry. As already observed for peptides containing benzophenone, the Pen(Lys48Bz) analogue was mainly unaffected by irradiation in ammonium acetate buffer. Pen(Lys48DTK) was strongly oxidized as a consequence of the irradiation, MALDI-TOF spectra showing the incorporation of one to four oxygen atoms. Pen(Lys48TMD) was nearly totally oxidized but with the incorporation of a single oxygen atom (+16).

The polar heads of phospholipids represent a borderline between two media, with a high dielectric constant (ε = 80, i.e., the aqueous phase) and a low dielectric constant (ε = 3, i.e., the lipid phase). This interface can be mimicked by glycerol (ε = 40). Glycerol adducts were efficiently formed with Pen(Lys48Bz), since a signal with a mass increase of 92 was observed. The signal intensity of the photoadduct was shown to increase as a function of the irradiation time (Figure 2). The disappearance as a function of time of the starting peptide Pen(Lys48Bz) (bearing four deuterated glycines) was quantified by addition after the irradiation of an internal standard (2 pmol) of Pen(Lys48Bz) (bearing four hydrogenated glycines) (*21*). The intact peptide remaining after irradiation was measured by integrating the ^{1}H and ^{2}H *m*/*z* signals (2864.3 and 2872.4, respectively), revealing an almost linear decrease of the starting material (Figure 2) as a function of the irradiation time. In the case of Pen(Lys48TMD), a mass increase of only 90, instead of 92, was observed, which probably resulted from the alcohol oxidation of the glycerol adduct. For Pen(Lys48TMD), the starting peptide and the photoadduct coexisted with the mono- and dioxidized forms. Weak signals were detected for Pen(Lys48DTK)

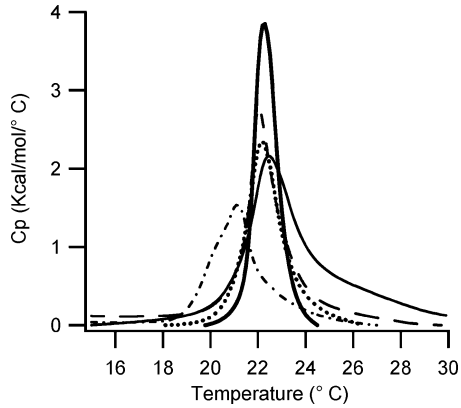

Figure 1. High-sensitivity DSC heating scans. The spectra illustrate the effect of adding penetratin (-•-) and penetratin photoactivatable analogues: Pen(LysBz) (••••), Pen(LysDTK) (- -), and Pen(LysTMD) (—) on the thermotropic phase behavior of DMPG multilamellar vesicles (— bold) at P/L of 1/25. Thermodynamic parameters are given in Table 1.

with a limited number of oxidized states compared to those observed in aqueous solution.

Finally, the reactivity of the photoactivatable penetratin analogues in a lipophilic medium was mimicked by photoirradiation of the peptides in SDS solution. In that environment, very low levels of cross-linking were detected, regardless of the photoprobe used. A small photoadduct signal was only observed for Pen(Lys48TMD). However, a high percentage of peptide oxidation was observed after irradiation under these conditions.

Analysis of the Photoadducts Obtained after Irradiation of Peptides with Phospholipid Bilayers. No photoadduct was observed by mass spectrometry after irradiation of DMPG vesicles in the presence of photoactivatable penetratin analogues, both using a crude preparation and after the purification step with streptavidin-coated magnetic beads. In order to observe photoadducts, the lipid moiety (hydrophobic character) of the adducts had to be removed by basic hydrolysis, which was performed overnight with NaOH (0.1 mol/L) in MeOH/H_2O (50/50) at 37 °C, followed by neutralization with acetic acid. MALDI-TOF mass spectrometry analysis was performed after a subsequent capture with streptavidin-coated magnetic beads in the presence of Triton X-100 (0.1%), followed by the described washing procedure and elution using the 2,5-dihydroxybenzoic acid matrix (*21*).

Photolabeling experiments with Pen(Lys48Bz) (2864.1) and DMPG vesicles led to three pairs of signals: one pair (3092.3 and +16) corresponding to photoadduct with the myristoyl and its oxidized form (+ 228 and + 244, respectively); another pair (2922.1 and +16) that was assigned to the dehydrated form of glycerol adducts formed during the basic treatment, and the third pair corresponding to the starting peptide and its oxidized form. Similar behavior and photoadducts were observed with Pen(Lys48TMD). Besides the oxidized form of Pen(Lys48TMD), previously observed in ammonium acetate buffer, two pairs of signals were detected, corresponding to mass increases of 228 and 72, which were assigned to photoadducts of myristoyl and oxidized/dehydrated glycerol, respectively. Finally, only degraded (low-molecular weights) forms of Pen(Lys48DTK) were detected after irradiation with DMPG vesicles (Figure 3).

Effect on the Organization of the Phospholipid Bilayer. DSC is used to study peptide/lipid interaction by monitoring the ability of peptides to interact and perturb the lipid acyl chain packing (Figure 1). A lipid bilayer composed of a single phospholipid, in the presence of water excess, can undergo two phase transitions upon heating: pretransition and main phase transition occurring at phase transition temperatures T_p and T_m (*29*). The peak area corresponds to the enthalpy of the phase transitions and the $\Delta H/T_m$ ratio to the entropy change. The main phase transition is related to the chain melting during the gel-to-liquid-crystalline phase change, whereas the pretransition reflects changes in headgroup tilting and organization.

In agreement with previous studies, the addition of the cationic peptide, penetratin, to anionic DMPG phospholipids suppressed the pretransition temperature and decreased both the enthalpy and the phase transition temperature (T_m) of the main lipid transition (*30*). One would expect that the introduction of hydrophobic probes in penetratin might promote the insertion of the peptide into the lipid fatty acid chains and so lead to an increased perturbation in the lipid phase transition. This was not the case; indeed, the photoactivatable probes did not significantly change the T_m and overall led to a smaller perturbation in the main phase transition compared to the original penetratin peptide. When comparing the three photoactivatable analogues, Pen(Lys48DTK) perturbed least the pretransition (that was not completly abolished) and main phase transition, leading to a very small reduction in the enthalpy of transition (Table 1). Altogether, the results demonstrate that the introduction of the photoactivatable probes in penetratin did not perturb the overall membranotropic properties of the peptide.

DISCUSSION

All experiments were performed in air-saturated water, in order to mimic the cellular environment. It has to be noted that, in the experiments described herein, 10 nmol of peptide was irradiated in the presence of about 90 nmol of oxygen (air-saturated water). Oxygen or water must be the first source(s), which might prevent the bimolecular photo-cross-linking of the photoactivated probes. The lifetime of the benzophenone triplet is 1.5 μs in air-saturated water, and much longer (20 μs) in degassed water (*31*). Oxygen efficiently quenches the benzophenone triplet by energy transfer, leading to the reactive singlet oxygen species with a short lifetime 4.2 μs in water (*32*), and its deactivation occurs by light emission and electronic-to-vibrational energy transfer and by intermolecular interaction with specific amino acids such as Phe or Trp, which are both present in penetratin (*33*). The benzophenone triplet can also be quenched by intra- or intermolecular interactions, by charge transfer, hydrogen abstraction, or light emission. However, all these reactions are fast and reversible, with the exception of the hydrogen abstraction step. The concentrations of the two active forms, i.e., the ketone triplet and the singlet oxygen, must be low under the irradiation conditions used herein, since the consumption of the starting peptide is slow (total disappearance occurs in over 2 h under permanent irradiation). For the dithienyl ketone triplet in air-saturated water, a large proportion of oxidized forms was observed showing that the singlet oxygen concentration must be much higher than for the benzophenone triplet. The carbene generated from trifluoromethylaryldiazirines has a very short lifetime ($t_{1/2} \approx$ ns) (*34*) because it reacts rapidly and irreversibly with oxygen. However, this competitive reaction with oxygen does not totally prevent the hydrogen abstraction, which can either occur intra- or intermolecularly.

With the benzophenone-substituted penetratin analogue, we have shown that the gradual decrease as a function of time up to the total disappearance of the starting peptide is slow. The intermolecular self-reaction is unlikely since no dimer was observed by MALDI-TOF MS (data not shown). The intramolecular reactions (hydrogen abstraction and radical combination) leading to cyclic peptides cannot be excluded with the techniques used. Photo-cross-linking with other species has already been reported for hydrophobic molecules (peptides, fatty acids,

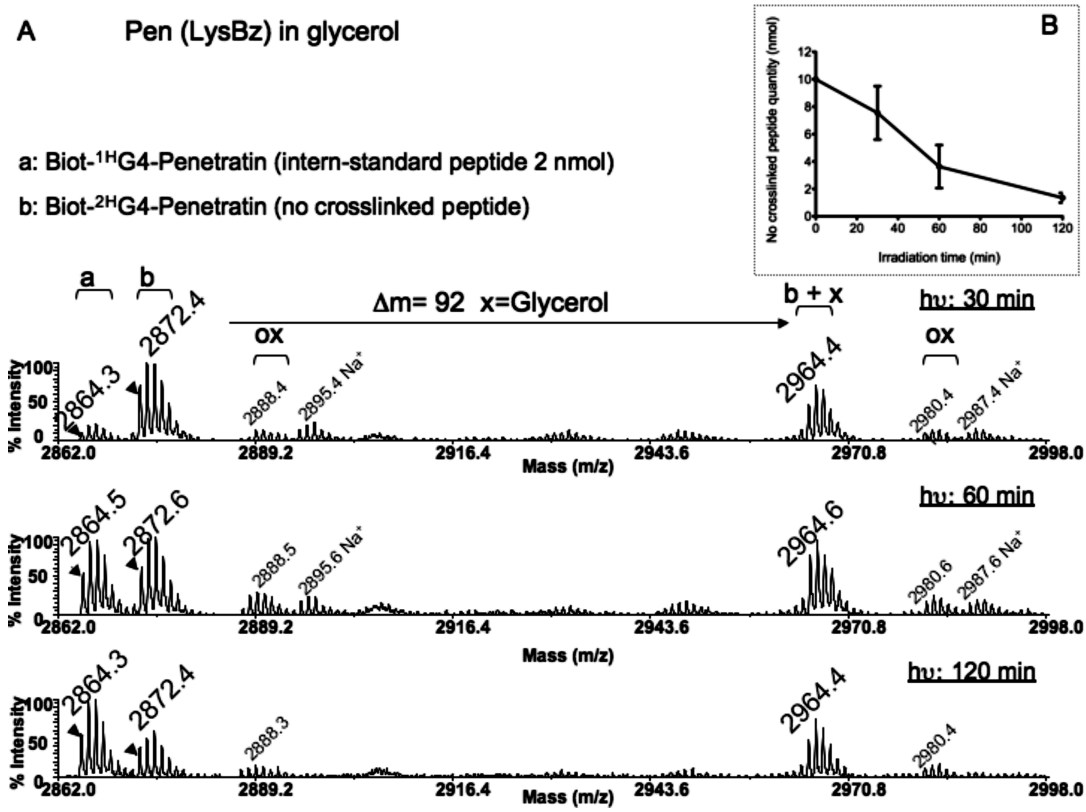

Figure 2. Quantification of remaining Pen(Lys48Bz) by MALDI-TOF mass spectrometry, after different irradiation times (30, 60, and 120 min irradiation) in glycerol. Insert top right, quantification of the areas of B vs A. A corresponds to 2 pmol of the peptide with four hydrogenated glycines added after the irradiation as an internal standard, the irradiation being performed with the same peptide bearing four deuterated glycines; *m/z* correspond to peaks B. For the capture by streptavidin-coated magnetic beads and the detection by MALFDI-TOF mass spectrometry as described in the experimental section.

Table 1. Thermodynamic Parameters Obtained by DSC for the Interaction of Penetratin and Its Photoactivatable Analogues with DMPG MLVs at P/L of 1/25

	pretransition		main transition	
	ΔH (kcal/mol)	T_p (° C)	ΔH (kcal/mol)	T_m (° C)
lipid alone	0.4	9.6	6.2	22.3
penetratin	−[a]	−	3.8	22.1
Pen(LysBz)	−	−	4.6	22.3
Pen(LysDTK)	0.2	8.8	6	22.1
Pen(LysTMD)	−	−	8	22.5

[a] − the transition was abolished.

phospholipids, glycolipids) soluble/inserted into a lipophilic phase, such as micelles or vesicles (*8, 14, 35*−*38*). A pioneer work has been reported on the labeling of "lipid mimics", i.e., sodium dodecylsulfate (SDS) micelles, with 10 mM benzophenone, using a 1/1 molar ratio (*35*). The very high peptide concentration and peptide/lipid ratio used in this study allowed the observation of the radical combination step, even though SDS exchange between micelles and free components and molecular motion (τ_c between 10^{-10} and 10^{-12} s) is a fast process ($t_{1/2} = 10^{-7}$ s) (*39*). Because the biological effects of membrane active peptides are generally observed at micromolar concentration and P/L ratios of ∼1/50, cross-linking experiments presented here have been performed at micromolar concentrations.

No efficient cross-linking was observed between the three tested photoactivatable peptides, at micromolar concentration in the presence of SDS micelles. These results suggest that a high concentration of photoreactive species is required to compensate the fast dynamics of supramolecular assemblage of SDS in micelles.

However, using DMPG vesicles and also micromolar concentrations of photoactivatable Pen(Lys48Bz) or Pen(Lys48TMD), phospholipid photoadducts were detected, even if the lateral diffusion in the disordered lamellar phase is around $10^{-7} > T_D < 5.10^{-9}$ cm^2.s^{-1} (*40*) with fast phospholipid motion (10^{-12} to 10^{-7} s) and fast exchange between free and bound peptide (with a dissociation constant in the micromolar range). The combination reaction occurs at time scales (10^{-6} s) slower than most phospholipid motion. Thus, the detection of photo-cross-linking with DMPG vesicles indicates the following: (i) cooperative diffusion of the penetratin photoactivatable analogues and the surrounding anionic phospholipids and (ii) restricted motion of the anionic phospholipids.

In a polar microenvironment such as glycerol, the triplet radical state can react by energy transfer like a photosensitizer, which, in the presence of oxygen, leads to the formation of singlet state oxygen. Finally, in a lipophilic medium the triplet radical might react with compounds possessing carbon-bound removable hydrogen atoms, which function as a quencher, as long as the intrinsic movements of the two molecules are slow enough to allow radical combination (DMPG). The cross-linking yield with trifluoromethylaryldiazirines, Pen(Lys48TMD), was also relatively low due to a competitive reaction, the carbene leading to a fast irreversible reaction with oxygen. The oxidation and β-elimination of the polar headgroups by basic hydrolysis prevent the assignment of the exact structures of the photoadducts. Finally, the triplet radical of dithienylketone, Pen(Lys48DTK), must act as a photosensitizer, regardless of the medium, since only oxidized and degraded species (lower molecular mass species) were found.

Thus, among the three photoprobes tested herein, only benzophenone (Bz) and trifluoromethylaryldiazirine (TMD) led to covalent bond formation with lipids, which were identifiable

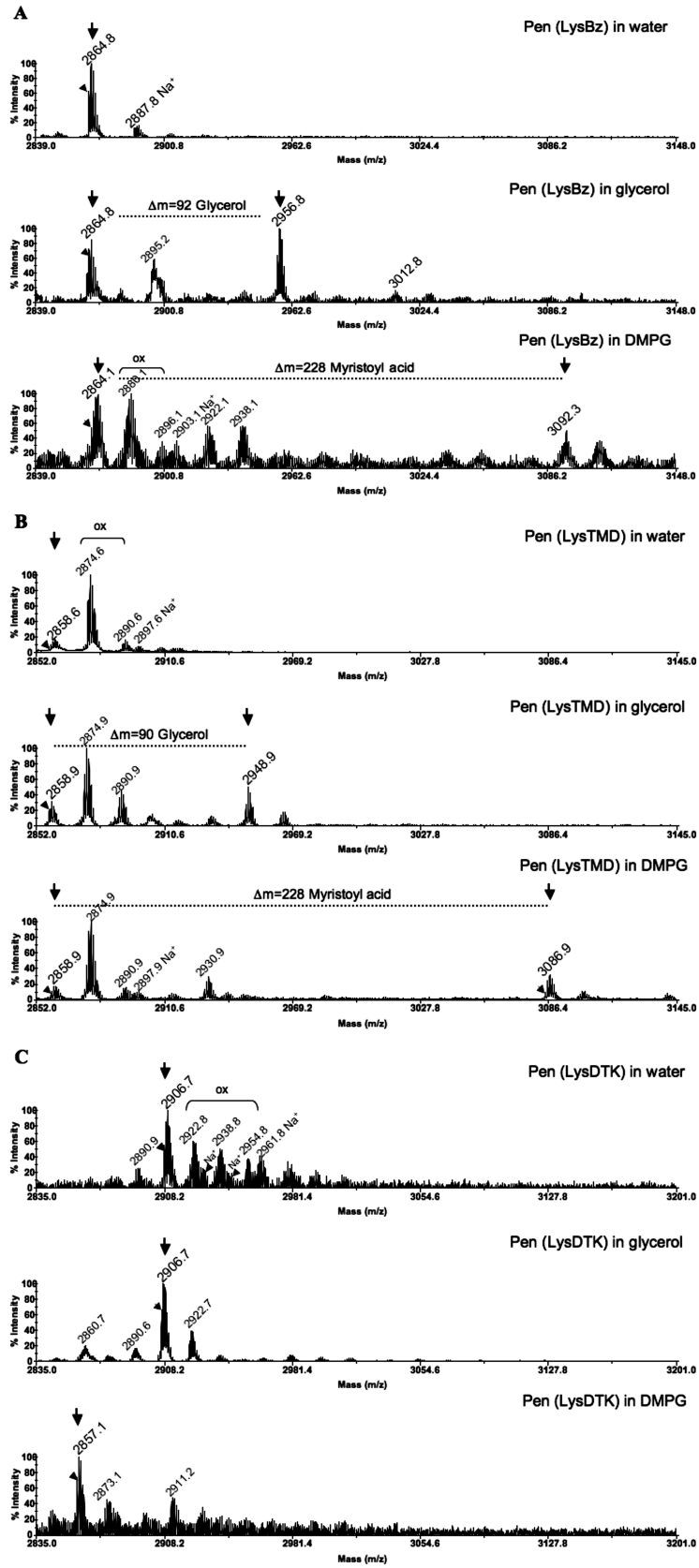

Figure 3. MALDI-TOF mass spectra of Pen(Lys48Bz) (A), Pen(Lys48DTK) (B), and Pen(Lys48TMD) (C) obtained after irradiation in water, glycerol, and DMPG vesicles. Pen(Lys48Bz), Pen(Lys48DTK), or Pen(Lys48TMD) dissolved at micromolar concentration in water or glycerol (500 μL) was irradiated on ice for 1 h at 365 nm. Then, 1 μL of the irradiated sample was deposited on the sample holder for MALDI-TOF mass spectrometry analysis. DMPG (1 mg/mL) was mixed with Pen(Lys48Bz), Pen(Lys48DTK), or Pen(Lys48TMD) at 1/25 peptide/lipid ratio. Theses samples were irradiated on ice for 1 h, at the same conditions as above, followed by an overnight basic hydrolysis. The hydrolyzed sample containing 0.1% of Triton was incubated with streptavidin-coated magnetic beads (100 μg, Dynabeads M280, Dynal). The same procedure was used for the experiments performed in SDS, except that no Triton was added during the incubation step. After different steps of washings, the photoadducts were eluted from the magnetic beads with the 2,5-dihydroxybenzoic acid (DHB) matrix. After 10 min incubation, 1 μL of bead-free supernatant was deposited on the sample holder for MALDI-TOF mass spectrometry analysis.

by MALDI-TOF mass spectrometry. Benzophenone (Bz) appeared to be the most appropriated photoprobe compared to TMD, since Bz leads to similar phase transition effects to those of penetratin, while TMD leads to great changes in the cooperativity of the transition, suggesting that TMD probably inserts deeper into the fatty acid chain region.

CONCLUSION

Herein, the photo-cross-linking of three photoactivatable penetratin peptides in glycerol, SDS, and lipid (DMPG) was evaluated. The dynamics of both SDS and the SDS/penetratin assemblies and the micromolar concentration of photoactivatable penetratin analogues used (in the range of biologically active concentrations) prevented peptide cross-linking to SDS. Regarding glycerol and lipids, even though photo-cross-linking occurred in both cases, the direct MS analysis of the photoadducts formed upon irradiation of the three different photoactivatable penetratin analogues was only achieved in the first one. The characterization of the photoadducts formed after lipid irradiation required basic hydrolysis of the lipid before extraction; otherwise, the capture with streptavidin-coated magnetic beads was ineffective. Bilayers of DMPG were photo-cross-linked with penetratin analogues, containing either benzophenone or trifluoromethylaryl diazirines but not phenylketone. With both photoactivatable penetratin analogues, MALDI-TOF analysis of the photoadducts formed after irradiation of the peptides with DMPG allowed unambiguous identification of the covalent bond formed with this lipid. Therefore, these analogues can be used to analyze the specific lipid(s) recruitment by penetratin, which represents an essential step in the understanding of the translocation mechanism of this cationic cell-penetrating peptide.

ACKNOWLEDGMENT

This work was supported by the Association Nationale pour la Recherche (ANR-Prob DOM). We thank the Pr. Gilbert Kirsch and his co-workers from the "Laboratoire d'Ingénierie Moléculaire et Biochimie Pharmacologique" Metz, France, for the generous gift of 5-carboxy-5′-methyl-2,2′-dithienylketone.

LITERATURE CITED

(1) Park, E. J., Carroll, G. T., Turro, N. J., and Koberstein, J. T. (2009) Shedding light on surfaces using photons to transform and pattern material surfaces. *Soft Matter 5*, 36–50.
(2) Dormán, G., and Prestwich, G. D. (2000) Using photolabile ligands in drug discovery and development. *TIBTECH 18*, 64–76.
(3) Brunner, J. (1996) Use of photocrosslinkers in cell biology. *Trends Cell Biol. 6*, 154–157.
(4) Kotzyba-Hibert, F., Kapfer, I., and Goeldner, M. (1995) Recent trends in photoaffinity labeling. *Angew. Chem., Int. Ed. 34*, 1296–1312.
(5) Fillion, D., Deraët, M., Holleran, B. J., and Escher, E. (2005) Stereospecific synthesis of a carbene-generating angiotensin ii analogue for comparative photoaffinity labeling: improved incorporation and absence of methionine selectivity. *J. Med. Chem. 48*, 3980–3990.
(6) Lequin, O., Bolbach, G., Fabrice, F., Convert, O., Girault-Lagrange, S., Chassaing, G., Lavielle, S., and Sagan, S. (2002) Involvement of the second extracellular loop (E2) of the neurokinin-1 receptor in the binding of substance P: Photoaffinity labeling and modeling studies. *J. Biol. Chem. 277*, 22386–22394.
(7) Jullian, V., Courtois, F., Bolbach, G., and Chassaing, G. (2003) Carbon-carbon bond ligation between cyclodextrin and peptide by photo-irradiation. *Tetrahedron Lett. 44*, 6437–6440.
(8) Ridder, A. N. J. A., Spelbrink, R. E. J., Demmers, J. A. A., Rijkers, D. T. S., Liskamp, R. M., Brunner, J., Heck, A. J. R., de Kruijff, B., and Killian, J. A. (2004) Photo-crosslinking analysis of preferential interactions between a transmembrane peptide and matching lipids. *Biochemistry 43*, 4482–4489.
(9) Maxfield, F. R. (2002) Plasma membrane microdomains. *Curr. Opin. Cell Biol. 14*, 483–487.
(10) Engelman, D. M. (2005) Membranes are more mosaic than fluid. *Nature 438*, 578–580.
(11) Lenne1, P.-F., Wawrezinieck, L., Fabien Conchonaud, F., Wurtz, O., Boned, A., Guo, X.-J., Rigneault, H., He, H.-T., and Marguet, D. (2006) Dynamic molecular confinement in the plasma membrane by microdomains and the cytoskeleton meshwork. *EMBO J. 25*, 3245–3256.
(12) Lagerholm, B. C., Weinreb, G. E., Jacobson, K., and Thompson, N. L. (2005) Detecting microdomains in intact cell membranes. *Ann. Rev. Phys. Chem. 56*, 309–333.
(13) Chachaty, C., Rainteau, D., Tessier, C., Quinn, P. J., and Wolf, C. (2005) Building up of the liquid-ordered phase formed by sphingomyelin and cholesterol. *Biophys. J. 88*, 4032–4044.
(14) Bino, J. B., Kumar, E. R., and Lala, A. K. (2000) Depth-dependent analysis of membranes using benzophenone-based phospholipids. *Biophys. Chem. 87*, 37–42.
(15) Coates Barclay, L. R., Baskin, K. A., Locke, S. J., and Schaefer, T. D. (1987) Benzophenone-photosensitized autoxidation of linoleate in solution and sodium dodecyl sulfate micelles. *Can. J. Chem. 65*, 2529–2540.
(16) Zhu, W. L., and Shin, S. Y. (2009) Antimicrobial and cytolytic activities and plausible mode of bactericidal action of the cell penetrating peptide penetratin and its Lys-linked two-stranded peptide. *Chem. Biol. Drug Des. 73*, 209–15.
(17) Palm, C., Netzereab, S., and Hällbrink, M. (2006) Quantitatively determined uptake of cell-penetrating peptides in non-mammalian cells with an evaluation of degradation and antimicrobial effects. *Peptides 27*, 1710–6.
(18) Balayssac, S., Burlina, F., Convert, O., Bolbach, G., Chassaing, G., and Lequin, O. (2006) Comparison of penetratin and other homeodomain-derived cell-penetrating peptides: interaction in a membrane-mimicking environment and cellular uptake efficiency. *Biochemistry 45*, 1408–1420.
(19) Christiaens, B., Symoens, S., Vanderheyden, S., Engelborghs, Y., Joliot, A., Prochiantz, A., Vandekerckhove, J., Rosseneu, M., and Vanloo, B. (2002) Tryptophan fluorescence study of the interaction of penetratin peptides with model membranes. *Eur. J. Biochem. 269*, 2918–2926.
(20) Christiaens, B., Grooten, J., Reusens, M., Joliot, A., Goethals, M., Vandekerckhove, J., Prochiantz, A., and Rosseneu, M. (2004) Membrane interaction and cellular internalization of penetratin peptides. *Eur. J. Biochem. 271*, 1187–1197.
(21) Burlina, F., Sagan, S., Bolbach, G., and Chassaing, G. (2005) Quantification of the cellular uptake of cell-penetrating peptides by MALDI-TOF mass spectrometry. *Angew. Chem., Int. Ed. 44*, 4244–4247.
(22) Aussedat, B., Sagan, S., Chassaing, G., Bolbach, G., and Burlina, F. (2006) Quantification of the efficiency of cargo delivery by peptidic and pseudo-peptidic trojan carriers using MALDI-TOF mass spectrometry. *Biochem. Biophys. Acta 1758*, 375–383.
(23) Delaroche, D., Aussedat, B., Aubry, S., Chassaing, G., Burlina, F., Clodic, G., Bolbach, G., Lavielle, S., and Sagan, S. (2007) Tracking a new cell-penetrating peptide, (RW)9, through an enzyme-stable mass spectrometry reporter. TAG. *Anal. Chem. 79*, 1932–1938.
(24) Magzoub, M., Eriksson, L. E., and Gräslund, A. (2002) Conformational states of the cell-penetrating peptide penetratin when interacting with phospholipid vesicles: effects of surface charge and peptide concentration. *Biochim. Biophys. Acta 1563*, 53–63.
(25) Binder, H., and Lindblom, G. (2003) Charge-dependent translocation of the Trojan peptide penetratin across lipid membranes. *Biophys. J. 85*, 982–95.
(26) Brunner, J., Senn, H., and Richards, F. M. (1980) 3-Trifluoromethyl-3-phenyldiazirine a new carbene generating group for photolabeling reagents. *J. Biol. Chem. 255*, 3313–3318.

(27) Nassal, M. (1983) 4-(1-Azi- 2,2,2-trifluoroethyl)benzoic acid a highly photolabile carbene generating label readly fixable to biochemical agents. *Liebigs Ann. Chem.* 1510–1523.
(28) Derossi, D., Joliot, A. J., Chassaing, G., and Prochiantz, A. (1994) The third helix of the Antennapedia homeodomain translocates through biological membranes. *J. Biol. Chem. 269*, 10444–10450.
(29) McElhaney, R. N. (1986) Differential scanning calorimetric studies of lipid-protein interactions in model membrane systems. *Biochim. Biophys. Acta 864*, 361–421.
(30) Alves, I. D., Goasdoué, N., Correia, I., Aubry, S., Galanth, C., Sagan, S., Lavielle, S., and Chassaing, G. (2008) Membrane interaction and perturbation mechanisms induced by two cationic cell penetrating peptides with distinct charge distribution. *Biochim. Biophys. Acta 1780*, 948–959.
(31) Canonica, S., Hellrung, B., and Wirz, J. (2000) Oxidation of Phenols by Triplet Aromatic Ketones in Aqueous Solution. *J. Phys. Chem. A 104*, 1226–1232.
(32) Rodgers, M. A. J. (1983) Solvent-induced deactivation of singlet oxygen: additivity relationships in nonaromatic solvents. *J. Am. Chem. Soc. 105*, 6201–6205.
(33) Harada, Y., Suzuki, K., Hashimoto, M., Tsukagoshi, K. and H., and Kimoto, H. (2009) Chemiluminescence from singlet oxygen that was detected at two wavelengths and effects of biomolecules on it. *Talanta 77*, 1223–1227.
(34) Gaudin, Y., Ruigrok, R. W. H., and Brunner, J. (1995) Low-pH induced conformational changes in viral fusion proteins: implications for the fusion mechanism. *J. Gen. Virol. 76*, 1541–1556.
(35) Breslow, R., Kitabatake, S., and Rothbard, J. (1978) Photoreactions of charged benzophenone with amphiphiles in micelles and multicomponent aggregates as conformational probes. *J. Am. Chem. Soc. 100*, 8156–8160.
(36) Delfino, J. M., Schreiber, S. L., and Richards, F. M. (1993) Design, synthesis, and properties of a photoactivatable membrane-spanning phospholipidic probe. *J. Am. Chem. Soc. 115*, 3458–3474.
(37) Lala, A. K., and Kumar, E. R. (1993) Orientation of the benzophenone group at various depths in bilayers. *J. Am. Chem. Soc. 115*, 3982–3988.
(38) Wendeler, M., Hoernschemeyer1, J., Hoffmann, D., Kolter, T., Schwarzmann, G., and Sandhoff, K. (2004) Photoaffinity labeling of the human GM2-activator protein mechanistic insight into ganglioside GM2 degradation. *Eur. J. Biochem. 271*, 614–627.
(39) Barker, C., Saul, D., Tiddy, G., Wheeler, B., and Willis, E. (1974) Phase structure, nuclear magnetic resonance and. rheological properties of viscoelastic sodium. dodecyl sulphate and trimethylammonium bromide mixtures. *J. Chem. Soc., Faraday Trans 1 70*, 154–162.
(40) Jain, M. K., and White, H. B. (1977) Long-range order in biomembranes. *Adv. Lipid Res. 15*, 1–60.

BC900466Q